A spatially implicit model fails to predict the structure of spatially explicit metacommunities under high dispersal

Ai, Dexiecuo; Ellwood, M. D. Farnon

Ecological Modelling

DOI:
https://doi.org/10.1016/j.ecolmodel.2022.110151

Published: 01/12/2022

Peer reviewed version

A spatially implicit model fails to predict the structure of spatially explicit metacommunities under high dispersal

Dexiecuo Ai[1*] and M. D. Farnon Ellwood[2]

[1]State Key Laboratory of Grassland Agro-Ecosystems, College of Ecology, Lanzhou University, Lanzhou, 730000, China. E-mail: aidxc@lzu.edu.cn

[2]School of Natural Sciences, Bangor University, Bangor, Gwynedd, LL57 2DG, United Kingdom. E-mail: farnon.ellwood@bangor.ac.uk

[*]Corresponding author

Abstract

Metacommunities are the product of species dispersal and topology. Metacommunity studies often use spatially *implicit* models, implemented by fully connected topologies, in which the precise spatial arrangement of habitat patches is not specified. Few studies use spatially *explicit* models, even though real-world metacommunities are likely structured by topology. Here, we test whether a spatially implicit resource consumption model based on a fully connected topology could predict the structure of spatially explicit metacommunities. Having controlled for environmental heterogeneity, we focus specifically on the effects of species dispersal and topology on metacommunity structure. We classified the topologies according to the shortest path between the most distant nodes (i.e. the graph diameter). Topologies with small diameters are tightly connected, whereas large diameter graphs are loosely connected. Some general trends emerged with increasing dispersal rate, such as a hump-shaped pattern in α-diversity, and a plateau followed by a decline in γ- diversity. However, the importance of topology was also apparent: α-diversity peaked at low dispersal rates in small diameter topologies, but at high dispersal rates in large diameter topologies. At low dispersal rates, α-diversity was higher in spatially implicit than in spatially explicit metacommunities. At medium dispersal we detected stronger species

sorting in the small diameter than in the large diameter topologies. Increasing dispersal caused α-diversity to decline more dramatically in small diameter topologies. Smaller metacommunities were dominated by regional competitors, whereas larger communities exhibited patterns of species biomass distribution leading to emergent niche structures. Increasing dispersal caused the mean productivity of each patch to undergo partial declines in spatially implicit metacommunities but continue to decline sharply in spatially explicit metacommunities. We conclude that spatially implicit models should be used cautiously when predicting the biodiversity, community composition or ecosystem functions of spatially explicit metacommunities at medium, and especially at high dispersal rates.

Key words: spatially implicit, spatially explicit, metacommunity, topology, dispersal, diversity, productivity, community composition, resource-consumption model

1. Introduction

Metacommunity theory integrates local and regional community dynamics, relating biodiversity and ecosystem functions at different spatial scales (Leibold & Chase 2018; Thompson *et al.* 2020). Fundamental tenets of metacommunity theory include species dispersal and topology, which describes the spatial arrangement of patches (Leibold & Chase 2018).

Species dispersal determines the rate of species movement within and between ecological communities (Massol *et al.* 2017; Thompson & Fronhofer 2019; Thompson *et al.* 2020; Vilmi *et al.* 2021; Zhang *et al.* 2021). Leibold *et al.* (2017) conceptualized three types of dispersal: dispersal limitation, dispersal sufficiency and dispersal surplus. Dispersal limitation prevents species from reaching patches where their productivity is the highest (Mouquet *et al.* 2002; Leibold *et al.* 2017). Dispersal sufficiency, the product of species sorting, allows each species to find its optimum patch, which increases the α-diversity of individual patches and leads to high productivity (Loreau *et al.* 2003; Mouquet & Loreau 2003; Leibold *et al.* 2017). Dispersal surplus counteracts the effects of dispersal limitation and dispersal sufficiency: in the short term poor competitors are able to coexist within patches, but eventually mass effects allow the best overall competitors to dominate individual

patches, causing dramatic declines in both α- and γ- diversity, and reducing mean productivity (Loreau *et al.* 2003; Mouquet & Loreau 2003; Leibold *et al.* 2017). A key point is that theoretical studies of dispersal limitation, dispersal sufficiency and dispersal surplus have all been based on spatially implicit models, in which the precise spatial location of habitat patches was not specified in the model (Leibold *et al.* 2017; Suzuki & Economo 2021).

In theoretical studies, if the dispersal rate is set to zero, all patches are isolated from each other, no information is transferred, and the system is closed. When the system is open, dispersal depends on topology (Economo & Keitt 2008). Topology determines how patches are arranged in relation to one another (Economo 2011; Suzuki & Economo 2021). In the real world, topology describes the spatial distribution and connectedness of landscape patches, informing conservation strategies such as reserve size (Minor & Urban 2008; Van Teeffelen *et al.* 2012), and explaining spatial insurance effects, where species escape from competition in heterogeneous landscapes (Thompson *et al.* 2014). A second key point is that spatially implicit models always use fully-connected topologies in which all patches are connected directly with other patches (Loreau *et al.* 2003; Mouquet & Loreau 2003; Suzuki & Economo 2021). Real-world metacommunities, even those of relatively

80 simple natural microcosms such as ponds or epiphytes, are rarely this interconnected,
81 which raises the question of whether spatially implicit models can be used to predict
82 the structure of spatially explicit metacommunities. While some theoretical studies
83 have applied complicated topologies to fit experimental metacommunities (e.g.Hubert
84 *et al.* 2015; Thompson & Gonzalez 2017; Thompson *et al.* 2017), these topologies
85 were highly susceptible to disturbance, and extensions or modifications were
86 impossible.

87 An effective way to model the spatial topologies of metacommunities would
88 be to use graph theory (Newman 2003; Minor & Urban 2008). Relatively new to
89 metacommunity ecology, graph theory has been used extensively for the study of
90 computer networks (Minor & Urban 2008). Given that most studies of
91 metacommunities are based on resource consumption models (Loreau *et al.* 2003;
92 Shanafelt *et al.* 2015; Thompson & Gonzalez 2017; Thompson *et al.* 2017; Leibold &
93 Chase 2018), we used a resource consumption model and six simple topologies taken
94 from computing networks, i.e. fully connected (spatially implicit), star, line, ring,
95 lattice and tree structures (Fig.1). We asked whether, under different levels of species
96 dispersal, a spatially implicit model could predict trends in α- and γ- diversity,
97 community composition, ecosystem function, and even spatial variations in the α-

98 diversity and ecosystem function of different patches in any of the six different
99 topologies.
100 Whilst environmental heterogeneity affects the structure of metacommunities
101 (Leibold & Chase 2018; Ben-Hur & Kadmon 2020; Suzuki & Economo 2021;
102 Thompson *et al.* 2021), that is outside the scope of this study, and we therefore
103 controlled for environmental effects by assuming that, although environmental
104 conditions differ between patches, overall environmental heterogeneity would be the
105 same for all topologies. We anticipated that our spatially implicit model would predict
106 diversity, ecosystem function and community composition under low and high
107 dispersal rates. Species sorting under low dispersal would result in patches with
108 similar environmental conditions being dominated by the best competitor, leading to
109 consistent species composition, whereas dispersal surplus under high dispersal would
110 result in superior competitors dominating all metacommunities, again leading to
111 consistent composition (Loreau *et al.* 2003; Mouquet & Loreau 2003). Consequently,
112 mean productivity within each patch would also be consistent for all topologies with
113 similar environmental conditions. We believe relatively low dispersal rates prevented
114 local diversity from declining in the spatially explicit topologies of Suzuki and
115 Economo (2021) when they asked similar questions to us, but measured species

diversity patterns only. However, we also anticipated that our spatially implicit model would fail to predict diversity, ecosystem function, and community composition at intermediate dispersal rates because of variations in the relative strength of species sorting and mass effects in different topologies.

2. Methods

We use the resource-consumption model (Loreau *et al.* 2003; Gonzalez 2009; Gonzalez *et al.* 2009; Shanafelt *et al.* 2015), which allows environmental conditions to fluctuate with time, whilst maintaining species diversity. As in previous studies, we assume that all species compete for a single limited resource, such as nitrogen, and convert it into new biomass. Unlike previous studies, our model allows environmental conditions to differ between patches, as though each patch was a different landscape, but overall environmental conditions remain constant. Each species has an optimal environmental value. Superior competitors exhibit a close match between their optimal environmental values and the environmental conditions of a patch and will therefore consume large amounts of resource. All metacommunities consisted of the same number of patches, with the same levels of environmental heterogeneity. Different topologies differed only in the connections between patches in various topologies. We set the unit of each parameter as Shanafelt *et al.* (2015).

2.1 Resource-consumption model

In our resource-consumption model, biomass of species *i* on patch *j* at time *t*, $P_{ij}(t)$ (units as g) increases due to the presence of species converting resource into biomass. Mortality reduces biomass within a patch, as does species emigration from a patch. Biomass within a patch increases as species immigrate from other patches, defined as the solution of:

$$\frac{dP_{ij}(t)}{dt} = \underbrace{e_{ij}C_{ij}R_j(t)P_{ij}(t)}_{\text{new production}} - \underbrace{m_{ij}P_{ij}(t)}_{\text{mortality}} + \underbrace{a\sum_{k=1,k\neq j}^{M_j}\frac{P_{ik}(t)}{M_k}}_{\text{immigration}} - \underbrace{aP_{ij}(t)}_{\text{emigration}}. \quad (1)$$

$R_j(t)$ (unit as ml, to distinguish from the unit of biomass) is the limited resource on patch *j* at time *t*; it is supplied from outside of the metacommunity at each time interval and declines due to lost and species consumption, defined as the solution of:

$$\frac{dR_j(t)}{dt} = I_j - l_jR_j(t) - R_j(t)\sum_{i=1}^{S}C_{ij}P_{ij}(t). \quad (2)$$

We numbered all patches from 1 to N (*N* is the number of patches, dimensionless), and all species from 1 to S, where *S* (dimensionless) is the initial number of species. e_{ij} (g/ml) is the rate of species *i* converting the consumed resource into new biomass on patch *j*; C_{ij} (1/(g*h)) is the rate of species *i* consuming resource on patch *j*, defined as (Gonzalez *et al.* 2009):

$$C_{ij} = 0.15\left(1 - \frac{|H_i - E_j|}{1.5}\right) \quad (3),$$

where the baseline maximum consumption rate is 0.15(1/(g*h)), and it is scaled down based on the difference between H_i and E_j.

E_j (dimensionless) is environmental condition of patch *j*, defined as:

$$E_j = \begin{cases} 1, & j = 1 \\ E_{j-1} - 1/(N-1), & 2 \le j \le N \end{cases} \quad (4).$$

H_i (dimensionless) is the optimal environmental value of species *i*, defined as:

$$H_i = \begin{cases} 1, & i = 1 \\ H_{i-1} - 1/(S-1), & 2 \le i \le S \end{cases} \quad (5).$$

I_j (ml/h) and l_j (1/h) are the resource input and loss rate, respectively; m_{ij} (1/h) is the loss rate of biomass of species *i* on patch *j*; a (1/h) is the dispersal rate of species; for the sake of simplicity we assume that all species have the same a which determines the fraction of dispersers at each time interval; M_j is the number of patches connected with patch *j*.

Another popular, spatially implicit metacommunity model is Mouquet and Loreau (2003); the main difference between this model and our model is that in their model reproduction depends on dispersal rate, and only new species disperse. In our model, reproduction depends on the available resource, and all species have a chance to disperse.

2.2 Six simple topologies

We apply six simple topologies often seen in computer networks (Fig.1). A brief

introduction for each of them is as follows:

Fully connected topology All patches are connected, meaning that species from a patch can disperse to other patches via an edge. In the real world, constructing a fully connected metacommunity would be laborious and expensive because of the large number of edges ($\frac{N(N-1)}{2}$), and fully connected metacommunities are not easy to extend or modify. However, a fully-connected topology is the most reliable structure in the event that patches or edges are disturbed. We use this topology to represent a spatially implicit structure.

Star topology All patches are connected to a central patch (e.g. patch 1 in Fig.1), and species disperse from one patch to another through the central patch, meaning the central patch plays a buffering role. With the exception of the central patch, this topology is easy to extend and modify. The number of edges is (N-1). The star topology is less resistant to disturbance than the fully connected topology, because when an edge or the central patch is removed, connectivity is lost.

Lattice topology This type of topology is rarely seen in computer networks but is easy to design in experimental metacommunity studies. Lattice topologies are essentially grids, with patches located at the intersection of each edge. Patches are connected via several paths. If N patches are distributed as an $N_r \times N_c$ lattice (where N_r and N_c are

188 the number of patches in each row and column, respectively), then the number of
189 edges in this lattice is $N_r \times (N_c - 1) + (N_r - 1) \times N_c$. The lattice topology is more
190 resistant to disturbance because the system remains connected even when several
191 patches or edges are damaged.
192 *Tree topology* The tree topology has root patches, and each root patch has two child
193 patches in our model (see Fig. 1). Child patches can be added to a root patch which
194 has fewer than two child patches, but the child patches will become unconnected if
195 any root patches or edges are removed. The number of edges in this topology is *N*-1.
196 *Ring topology* Each patch connects with two neighboring patches, which together
197 form a ring shape. Species can disperse clockwise or counterclockwise (Meador 2008).
198 Either way, dispersers must pass through all patches located between the patch they
199 emigrate from and the patch they immigrate to (Meador 2008). This topology is easy
200 to set up, but the ring is temporarily broken during extension of the ring topology. The
201 number of edges is *N*. If more than one patch or edge are removed, the system
202 becomes unconnected.
203 *Line topology* In the line topology, the first and last patch are unconnected, so there is
204 only one route along which species can disperse. This structure is easy to extend but
205 less resistant to disturbance since it becomes unconnected when any of the

206 intermediate patches or edges are removed. The number of edges is *N*-1.

207 Topologies can be classified according to the number of edges of the shortest
208 path between the most distant nodes, known as the graph diameter (West 2001). The
209 diameters of our topologies can be classified into small, medium, and large groups:
210 the fully connected and star topologies had graph diameters of 1 and 2; the tree and
211 lattice topologies had diameters of 8 and 9; the ring and line topologies had diameters
212 of 15 and 29. Topologies with small diameters consist of a series of tight connections,
213 whereas larger graph diameters consist of loose connections.

214 **2.3 Simulations**

215 We set the number of patches to *N*=30 in all topologies and numbered each patch as in
216 Fig. 1. Environmental conditions, defined by equation (4), were consistent within
217 patches of a similar color, or numbered sequentially for different topologies. We set
218 the initial species richness to *S*=30 and numbered the species from 1 to 30, setting the
219 optimal environmental value of each species according to equation (5). All species
220 had the same e_{ij} and m_{ij} (both values set to 0.2) for all patches (Loreau *et al.* 2003;
221 Gonzalez *et al.* 2009), and all patches had the same I_j and l_j, values set to 165 and 10
222 respectively (Gonzalez *et al.* 2009). We set these parameters based on previous
223 studies which applied the resource-consumption model. We set the dispersal rate a to

37 different values, ranging from 0.0001 to 0.001 with intervals of 0.0001, ranging from 0.001 to 0.01 with intervals of 0.001, ranging from 0.01 to 0.1 with intervals of 0.01, and ranging from 0.1 to 1 with intervals of 0.1. Hence, we have 37 (dispersal rates) *6 (topologies) = 222 simulations, with each simulation run for 2*10^7 time steps to reach equilibrium. We set a dynamic cutoff at $P_{ij}(t) = 0.01$(g), meaning that species became extinct from a patch if their biomass fell below this value. The differential equations of (1) and (2) are simulated by using the forward Euler method with *dt*=0.001. We also tested the results for different *dt*, observing the same patterns when *dt* was relatively large, such as 0.005 and 0.01 (see the results of *dt*=0.01 in the Appendices), but the system was not at steady state when *dt* increased, for example greater than 0.1. We controlled for spatial heterogeneity using the fully connected (spatially implicit) topology, in which all patches were connected directly.

2.4 Metrics

We used the Bray-Curtis dissimilarity index to measure the community composition of each patch, comparing patches of the fully-connected topology with all other topologies. In addition, we measured the total biomass of each species (summing the biomass of that species across all patches) in the whole metacommunity, the α-diversity (number of species) within each patch, the γ-diversity of the

metacommunities, and the coefficient of variation (hereafter CV, defined as standard deviation/mean) of α-diversity across patches. We also measured the productivity of each patch *j* defined as the production of new biomass per unit time (g/h, Loreau *et al.* 2003):

$$\varphi_j(t) = R_j(t) \sum_{i=1}^{S} e_{ij} C_{ij}(t) P_{ij}(t). \quad (6)$$

As well as productivity per patch, we measured the cv of productivity between patches. Similations were implemented in Java, topologies and similarity of community composition were generated using the "igraph" and "vegan" packages in R, and data were analysed in R 4.0.4 (R 2021). All codes can be found in the Appendices.

3. Results

3.1 Community composition

Under low dispersal, strong species sorting appeared in all topologies (see *a*=0.0001 and *a*=0.001 in Fig.2). Under medium dispersal, mass effects increased the biomass of the inferior species, resulting in slight differences in community composition between topologies (see *a*=0.01 in Fig.2). However, the best competitor of the central patch in the star topology went extinct (i.e. in Fig.2 the color of the first species on the first patch is white when a=0.0001, but is red on all patches where *a*=0.01). Under high

dispersal in the fully connected, star, tree, and lattice topologies, whole metacommunities were dominated by a few species, and the optimal environmental values of these dominant species were located more centrally between 0 and 1 in the fully-connected topology than in the other topologies. In the line and ring topologies, species with extreme environmental values dominated the patches with extreme environmental conditions, whereas species with medium environmental values showed dominance in the patches with intermediate environmental conditions (see a=1 in Fig. 2). Overall, as the diameters of the topologies increased, dominant species exhibited more extreme environmental values.

We compared community composition between two patches with the same environmental conditions; one from the fully-connected topology, and the other from one of the other topologies. In all topologies, increasing disperal rates caused reduced similarity in community composition (Fig. 3). Low dispersal rates resulted in almost the same community composition within patches across all topologies (a=0.0001 in Fig. 3). Medium dispersal rates (e.g. a=0.01) increased the similarity between patches with extreme environmental conditions more than other patches. High dispersal rates (e.g. a=0.1) caused patches with intermediate environmental conditions to become more similar than patches with extreme environmental condititions. When the

278 dispersal rate was 1, the overall similarity was zero (Fig. 3). However, similarity was
279 greater than zero in the line and ring topologies (a=1 in Fig. 3). In contrast with the
280 other topologies, the similarity of patch 1 in the star topology was lowest when
281 dispersal rate was low, and highest when dispersal rate was 1 (Fig. 3).
282 At around 100, total biomass of each species in the whole metacommunity was
283 almost identical under low dispersal rates for all topologies (see a=0.0001 in Fig. 4).
284 It differed slightly under medium dispersal rates for the large-diameter topologies, but
285 remained the same for the fully-connected topology (see a=0.01 in Fig. 4). For the
286 star topology, the total biomass of species with environmental values of H=1 was zero
287 since they had been outcompeted as the best competitors of the central patch (patch 1,
288 see also Fig. 2). Total biomass differed greatly under high dispersal, especially for the
289 topologies with medium to large diameters, with clumps of species appearing as one
290 would expect from niche partitioning. The number of clumps increased from one to
291 four in the tree, lattice, ring and line topologies, respectively (a=1 in Fig. 4).
292 *3.2 Diversity*
293 In line with other studies (Loreau *et al.* 2003; Mouquet & Loreau 2003; Shanafelt *et*
294 *al.* 2015), increasing dispersal first increased and then decreased α-diversity, whereas
295 γ- diversity remained constant before eventually decreasing in all topologies (Fig.5A

296 and B). Exact trends of α- and γ-diversity varied between topologies. α-diversity was
297 highest (30 species) in the widest dispersal window of the fully-connected topology,
298 where the logarithm governing dispersal rates was between -7.5 to -2.5 (Fig.5A). The
299 same result could be seen in the star topology, but with a narrower dispersal window
300 (from -5.0 to -2.3) and a lower α-diversity (29 species). For the lattice and tree
301 topologies, medium dispersal rates gave the highest α-diversity, whereas in the line
302 and ring topologies α-diversity peaked at relatively higher dispersal rates. Also
303 dependent on topology were the tipping points at which γ- diversity started to decline.
304 At high rates of dispersal, both α- and γ- diversity were higher in the line and ring
305 topologies than in other topologies (Fig 5A and B).
306 α-diversity varied between patches in the different topologies (Fig.5C and Fig.
307 A.1). In all but the star topology, dispersal caused the cv of α-diversity to increase at
308 first and then decrease (Fig. 5C). The key difference between the topologies was the
309 point at which increasing dispersal caused the cv of α-diversity to peak. This peak
310 occurred at low dispersal in the fully-connected topology, intermediate dispersal in the
311 lattice and tree topologies, and high dispersal in the line and ring topologies (see
312 insert panels in Fig. 5C). In the star topology, which differed completely from the

313 other topologies, increasing dispersal caused a decline in the cv of α-diversity within
314 patches (Fig. 5C).

315 *3.3 Productivity*

316 Increasing dispersal caused the mean productivity of each patch to decrease in all
317 topologies, and the rate of decline became steeper at higher dispersal rates (Fig.6A,
318 see also the productivity of each patch across all topologies in Fig. A.2). In the fully
319 connected topology, even under very high dispersal rates, mean productivity remained
320 constant, whereas it declined sharply for the star topology, and remained relatively flat
321 in the line and ring topologies.

322 As with mean productivity, the cv of productivity between patches remained
323 constant at first, but then increased with dispersal in all but the fully-connected
324 topology (Fig. 6B), in which it declined slightly at very high dispersal rates. Under
325 high dispersal rates, the cv of productivity increased sharply in the star topology, and
326 remained flat in the line and ring topologies.

327 **4. Discussion**

328 We applied a resource-consumption model to six simple topologies: fully connected
329 (spatially implicit), star, tree, lattice, ring, and line structures with different diameters
330 to investigate whether a spatially implicit model could consistently predict the

331 structures of spatially explicit metacommunities. Under high dispersal, our spatially
332 implicit model failed to predict the structure of spatially explicit metacommunities,
333 including community composition, exact α- and γ- diversity, patterns of total species
334 biomass distribution, productivity, and cv of α-diversity and productivity. Some
335 trends were apparent across all models, for example at low dispersal, strong
336 environmental filtering led each patch to be dominated by its best competitor, whereas
337 more inferior competitors appeared in all patches at medium dispersal, and whole
338 metacommunities were dominated by several species due to mass effects at high
339 dispersal. Consequently, α-diversity first increased and then decreased, and γ-
340 diversity remained constant and then decreased.
341 At low dispersal (e.g. a=0.0001), community compositions of given patches
342 were consistent across topologies (Fig. 2-4) due to strong environmental filtering
343 which allowed each patch to be dominated by its best competitor (Suzuki & Economo
344 2021). γ- diversity and mean productivity were also consistent across all topologies,
345 and the cv of α-diversity between patches was low (Fig. 5 and 6). However, the high
346 levels of connectedness between patches in the fully connected topology allowed
347 more inferior species to appear in all patches even under very low dispersal rates,
348 which is why the α-diversity was higher under the fully connected topology than in

other topologies (Fig. 5). Our spatially implicit model could not predict the α-diversity of spatially explicit metacommunities, even under very low dispersal rates. Hence, α-diversity remained highest over the greatest range of dispersal in the fully connected topology than in other topologies. At medium dispersal (a=0.01), the number and identity of inferior species which appeared in each patch differed between patches and between topologies, which led the diversity and community composition to fluctuate within patches and topologies (Fig. 2-5), resulting in variable declines in productivity (Fig. 6, Mouquet & Loreau 2003; Leibold & Chase 2018). The central patch (patch 1) of the star topology represented a hub, meaning that all dispersers had to pass through this patch before reaching their destination, and these transient species converted resource and outcompeted the best competitor of the central patch.

At high dispersal, the smallest diameter topologies were dominated by generalist species with medium environmental values (Fig. 2). These species were also the best competitors at the regional scale, consistent with other studies (Mouquet & Loreau 2002; Loreau *et al.* 2003; Mouquet & Loreau 2003; Gonzalez *et al.* 2009; Shanafelt *et al.* 2015). Contrary to our expectations, increasing dispersal caused extreme shifts in the community compositions of medium to large diameter topologies. For example, the patches with extreme environmental conditions in the large-diameter

367 topologies were completely dominated by a few species with extreme environmental
368 values (Fig. 2). Fewer connections between patches meant that species could disperse
369 only to neighboring patches, particularly at high dispersal rates. This process led to
370 the emergent niche structure (Rael *et al.* 2018) observed in the large-diameter
371 topologies (Fig. 4). Patches with medium environmental conditions had similarities
372 greater than zero between the fully connected topology and the line and ring
373 topologies (Fig. 3), because generalist species with medium environmental values also
374 achieved greater biomass in patches with medium environmental conditions in the
375 line and ring topologies (Fig. 2). As we predicted, both α- and γ-diversity declined at
376 very high dispersal rates in all topologies, but greater numbers of species could be
377 maintained in the line and ring than in other topologies (Fig. 5), delaying the
378 reduction in productivity (Fig. 6). In the fully connected topology, the best regional
379 competitors dominated all patches at relative to very high dispersal rates, which kept
380 mean productivity constant and caused slight declines in the cv of productivity (Fig.
381 6).

382 Metacommunities are the product of complex interconnections between
383 species dispersal and network topologies, governed by environmental factors. Without
384 these interconnections, metacommunities would exist as random patches, rather than

being the products of species sorting and mass effects (Leibold *et al.* 2004; Suzuki & Economo 2021). Species sorting and mass effects work together, and the relative importance of these mechanisms for diversity is contingent upon dispersal rates and environmental filtering (Suzuki & Economo 2021). Environmental filtering and dispersal play opposite roles in community assembly: environmental filtering strengthens interspecific competition, allowing the best competitors to exclude less competitive species and dominante in each patch (Ben-Hur & Kadmon 2020); dispersal allows species to escape from competitive exclusion, appearing in patches where they could not survive without dispersal (Amarasekare & Nisbet 2001; Leibold *et al.* 2017). Regardless of topology, mass effects are proportional to species dispersal, whereas species sorting is the opposite in our model. Suzuki and Economo (2021) proposed that topologies with few loops promote species sorting, and we have confirmed this at high dispersal rates (Fig.2, Fig 4 and Fig. A.3). On the contrary, under medium dispersal rates (e.g., a=0.01 in Fig. 2 and 4), we found species sorting to be stronger in the small-diameter topologies such as the fully connected and star topologies than in the large-diameter topologies (see Fig.2, Fig 4 and Fig. A.3). Under high dispersal, the emergent niche structure of species biomass distribution patterns (Rael *et al.* 2018) appeared in topologies with large diameters, a similar feature to that

403 mentioned in Suzuki and Economo (2021). In previous studies, species traits dictated
404 whether niche structures emerged, further strengthening the heterogeneity of species
405 interactions (Rael *et al.* 2018). In our model, species trait differences were consistent
406 between topologies, but the spatial structure of the topologies altered the species
407 interactions.

408 Neither dispersal limitation nor dispersal sufficiency played a role in our
409 model. Only dispersal surplus was occurring, with all species appearing in all patches
410 from the start. Species sorting was at its most powerful when dispersal rate was zero
411 (Leibold & Chase 2018), and environmental conditions were filtering out the best
412 competitors from each patch. Our results appear to conflict with previous studies, in
413 which dispersal sufficiency always caused species sorting, and dispersal surplus
414 generated mass effects (Leibold *et al.* 2017; Leibold & Chase 2018). However, in
415 these studies, species were distributed randomly between patches, meaning that the
416 best competitors may not have existed in their preferred patches from the start. In
417 models like ours, all species have equal opportunities to appear in all patches from the
418 beginning.

419 *Conclusion* Our spatially implicit model successfully predicted community
420 composition, γ-diversity, and productivity at low dispersal rates for all topologies,

421 although α-diversity was higher in the spatially implicit than in any of the spatially
422 explicit topologies. At high dispersal rates, and given that the success of each
423 topology depends on the exact structure of metacommunities, none of these
424 characteristics were successfully predicted. Our aim was to test the resource-
425 consumption model under various assumptions, in the hope of suggesting a general
426 level of accuracy for this one spatially implicit model, and further tests involving
427 various other models and parameters are needed. In the meantime, we tentatively
428 conclude that spatially implicit models may be problematic in the study of spatially
429 explicit metacommunities, especially at high dispersal rates.

430 **5. Acknowledgements**

431 This study was supported by the National Natural Science Foundation of China
432 (No.31500336) and the Supercomputing Center of Lanzhou University. We thank
433 Juan A. Blanco and two anonymous reviewers for comments that improved the
434 manuscript.

435 **6. References**

436 Amarasekare, P. & Nisbet, R.M. (2001). Spatial heterogeneity, source-sink dynamics,
437 and the local coexistence of competing species. *Am Nat*, 158, 572-584.
438 Ben-Hur, E. & Kadmon, R. (2020). Heterogeneity–diversity relationships in sessile

organisms: a unified framework. *Ecology Letters*, 23, 193-207.

Economo, E.P. (2011). Biodiversity Conservation in Metacommunity Networks: Linking Pattern and Persistence. *The American Naturalist*, 177, E167-E180.

Economo, E.P. & Keitt, T.H. (2008). Species diversity in neutral metacommunities: a network approach. *Ecology Letters*, 11, 52-62.

Gonzalez, A. (2009). Metacommunities: Spatial Community Ecology. *eLS*.

Gonzalez, A., Mouquet, N. & Loreau, M. (2009). Biodiversity as spatial insurance the effects of habitat fragmentation and dispersal on ecosystem functioning. In: *Biodiversity, Ecosystem Functioning , and Human Wellbeing* (eds. Naeem, S, Bunker, D, Hector, A, Loreau, M & Perrings, C). Oxford University Press, pp. 134-146.

Hubert, N., Calcagno, V., Etienne, R.S. & Mouquet, N. (2015). Metacommunity speciation models and their implications for diversification theory. *Ecology Letters*, 18, 864-881.

Leibold, M., Chase, J.M. & Ernest, S.K.M. (2017). Community assembly and the functioning of ecosystems: how metacommunity processes alter ecosystems attributes. *Ecology*, 98, 909-919.

Leibold, M.A. & Chase, J.M. (2018). *Metacommunity Ecology, Volume 59*. Princeton

University Press.

Leibold, M.A., Holyoak, M., Mouquet, N., Amarasekare, P., Chase, J.M., Hoopes, M.F. *et al.* (2004). The metacommunity concept: a framework for multi-scale community ecology. *Ecology Letters*, 7, 601-613.

Loreau, M., Mouquet, N. & Gonzalez, A. (2003). Biodiversity as spatial insurance in heterogeneous landscapes. *Proceedings of the National Academy of Sciences*, 100, 12765-12770.

Massol, F., Altermatt, F., Gounand, I., Gravel, D., Leibold, M.A. & Mouquet, N. (2017). How life-history traits affect ecosystem properties: effects of dispersal in meta-ecosystems. *Oikos*, 126, 532-546.

Meador, B. (2008). A Survey of Computer Network Topology and Analysis Examples. Available at: https://www.cse.wustl.edu/~jain/cse567-08/ftp/topology/index.html.

Minor, E.S. & Urban, D.L. (2008). A Graph-Theory Framework for Evaluating Landscape Connectivity and Conservation Planning. *Conservation Biology*, 22, 297-307.

Mouquet, N. & Loreau, M. (2002). Coexistence in Metacommunities: The Regional Similarity Hypothesis. . *The American Naturalist*, 159, 420-426.

Mouquet, N. & Loreau, M. (2003). Community Patterns in Source‐Sink Metacommunities. *The American Naturalist*, 162, 544-557.

Mouquet, N., Moore, J.L. & Loreau, M. (2002). Plant species richness and community productivity: why the mechanism that promotes coexistence matters. *Ecology Letters*, 5, 56-65.

Newman, M.E.J. (2003). The Structure and Function of Complex Networks. *SIAM Review*, 45, 167-256.

R, C.T. (2021). R: A language and environment for statistical computing. R Foundation for Statistical Computing, Vienna, Austria. Available at: URL https://www.R-project.org/.

Rael, R.C., D'Andrea, R., Barabás, G. & Ostling, A. (2018). Emergent niche structuring leads to increased differences from neutrality in species abundance distributions. *Ecology*, 99, 1633-1643.

Shanafelt, D.W., Dieckmann, U., Jonas, M., Franklin, O., Loreau, M. & Perrings, C. (2015). Biodiversity, productivity, and the spatial insurance hypothesis revisited. *J Theor Biol*, 380, 426-435.

Suzuki, Y. & Economo, E.P. (2021). From species sorting to mass effects: spatial network structure mediates the shift between metacommunity archetypes.

493 *Ecography*, 44, 715-726.

494 Thompson, P.L. & Fronhofer, E.A. (2019). The conflict between adaptation and

495 dispersal for maintaining biodiversity in changing environments. *Proceedings*

496 *of the National Academy of Sciences*, 116, 21061.

497 Thompson, P.L. & Gonzalez, A. (2017). Dispersal governs the reorganization of

498 ecological networks under environmental change. *Nature Ecology & Evolution*,

499 1, 0162.

500 Thompson, P.L., Guzman, L.M., De Meester, L., Horváth, Z., Ptacnik, R.,

501 Vanschoenwinkel, B. *et al.* (2020). A process-based metacommunity

502 framework linking local and regional scale community ecology. *Ecology*

503 *Letters*, 23, 1314-1329.

504 Thompson, P.L., Kéfi, S., Zelnik, Y.R., Dee, L.E., Wang, S., de Mazancourt, C. *et al.*

505 (2021). Scaling up biodiversity-ecosystem functioning relationships: the role

506 of environmental heterogeneity in space and time. *Proceedings. Biological*

507 *sciences*, 288, 20202779.

508 Thompson, P.L., Rayfield, B. & Gonzalez, A. (2014). Robustness of the spatial

509 insurance effects of biodiversity to habitat loss. *Evolutionary Ecology*

510 *Research*, 16, 445-460.

511 Thompson, P.L., Rayfield, B. & Gonzalez, A. (2017). Loss of habitat and connectivity
512 erodes species diversity, ecosystem functioning, and stability in
513 metacommunity networks. *Ecography*, 40, 98-108.
514 Van Teeffelen, A.J.A., Vos, C.C. & Opdam, P. (2012). Species in a dynamic world:
515 Consequences of habitat network dynamics on conservation planning.
516 *Biological Conservation*, 153, 239-253.
517 Vilmi, A., Gibert, C., Escarguel, G., Happonen, K., Heino, J., Jamoneau, A. *et al.*
518 (2021). Dispersal–niche continuum index: a new quantitative metric for
519 assessing the relative importance of dispersal versus niche processes in
520 community assembly. *Ecography*, 44, 370-379.
521 West, D.B. (2001). *Introduction to Graph Theory. 2nd Edition, Prentice-Hall, Inc.,*
522 *Upper Saddle River, 82-83*.
523 Zhang, H., Bearup, D., Nijs, I., Wang, S., Barabás, G., Tao, Y. *et al.* (2021). Dispersal
524 network heterogeneity promotes species coexistence in hierarchical
525 competitive communities. *Ecology Letters*, 24, 50-59.
526
527

7. Figure captions

Figure 1 Six simple topologies were applied in our model; the number on each patch determines its environmental conditions, and the patches with similar colors have similar environmental conditions. Environmental conditions were consistent for all patches across all topologies. All topologies were classified into small diameter (fully connected and star topologies), medium diameter (lattice and tree topologies) and large diameter (line and ring topologies). D is the diameter of each topology.

Figure 2 The distribution of biomass of each species in each patch under various topologies and dispersal rates. The x-axis represents the patch and the y-axis is the species. White color denotes high biomass, whereas red color denotes low biomass.

Figure 3 The similarity of community composition between two patches with the same envionmental conditions under several dispersal rates; one patch is from the fully-connected topology and the other is from the other topologies.

Figure 4 The distribution of total biomass across species environmental values under various topologies and dispersal rates.

546

547 **Figure 5** Effects of dispersal on α-diversity (A), γ- diversity (B) and the coefficient of

548 variation of α-diversity across patches (C) in various topologies. To illustrate the

549 trends in cv of α-diversity for the line, ring, lattice and tree topologies, we replot a

550 nonlinear regression ($P<0.001$), inserted in panel C. The red, green and blue lines are

551 for topologies with small, medium and large diameters, respectively. The x-axis is

552 $\log_{10}$.

553

554 **Figure 6** Trends in mean productivity of each patch (A) and coefficient of variation of

555 productivity within patches (B) with dispersal for all topologies. The color scheme of

556 the lines is the same as in Figure 5. The x-axis is $\log_{10}$.

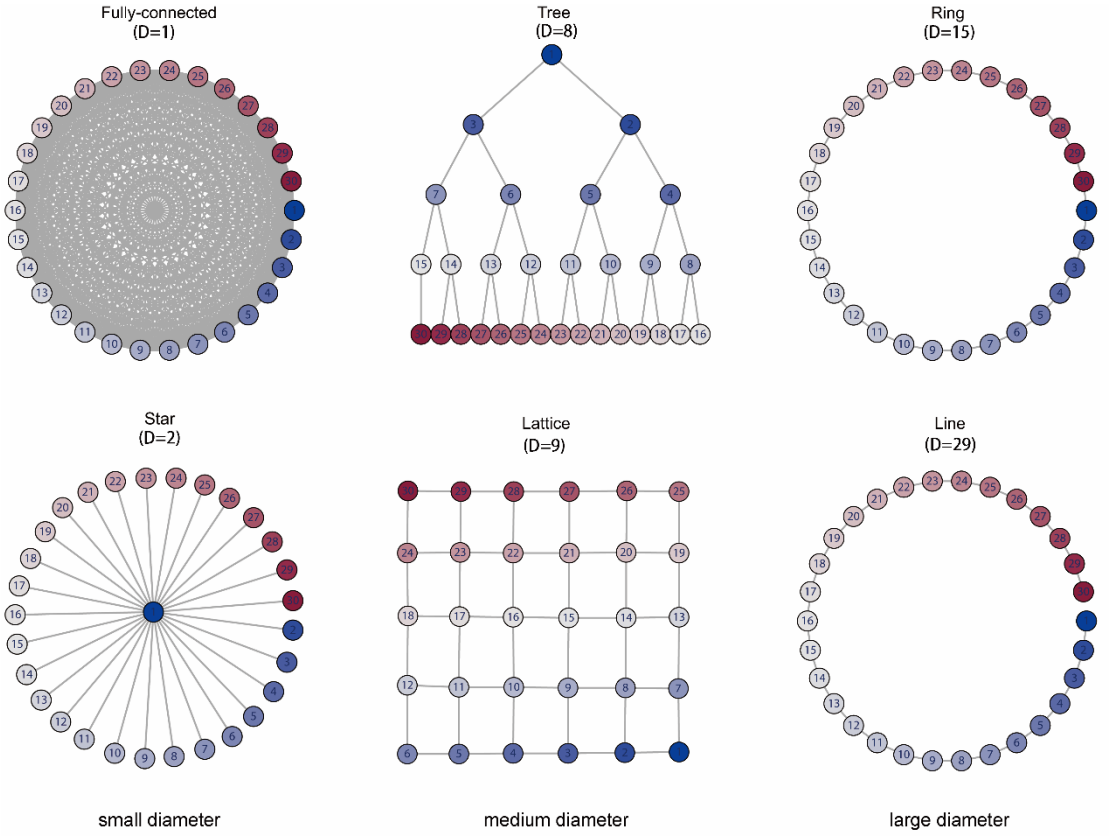
Fully-connected
(D=1)
Tree
(D=8)
Ring
(D=15)
Star
(D=2)
Lattice
(D=9)
Line
(D=29)
small diameter
medium diameter
large diameter

Figure 1

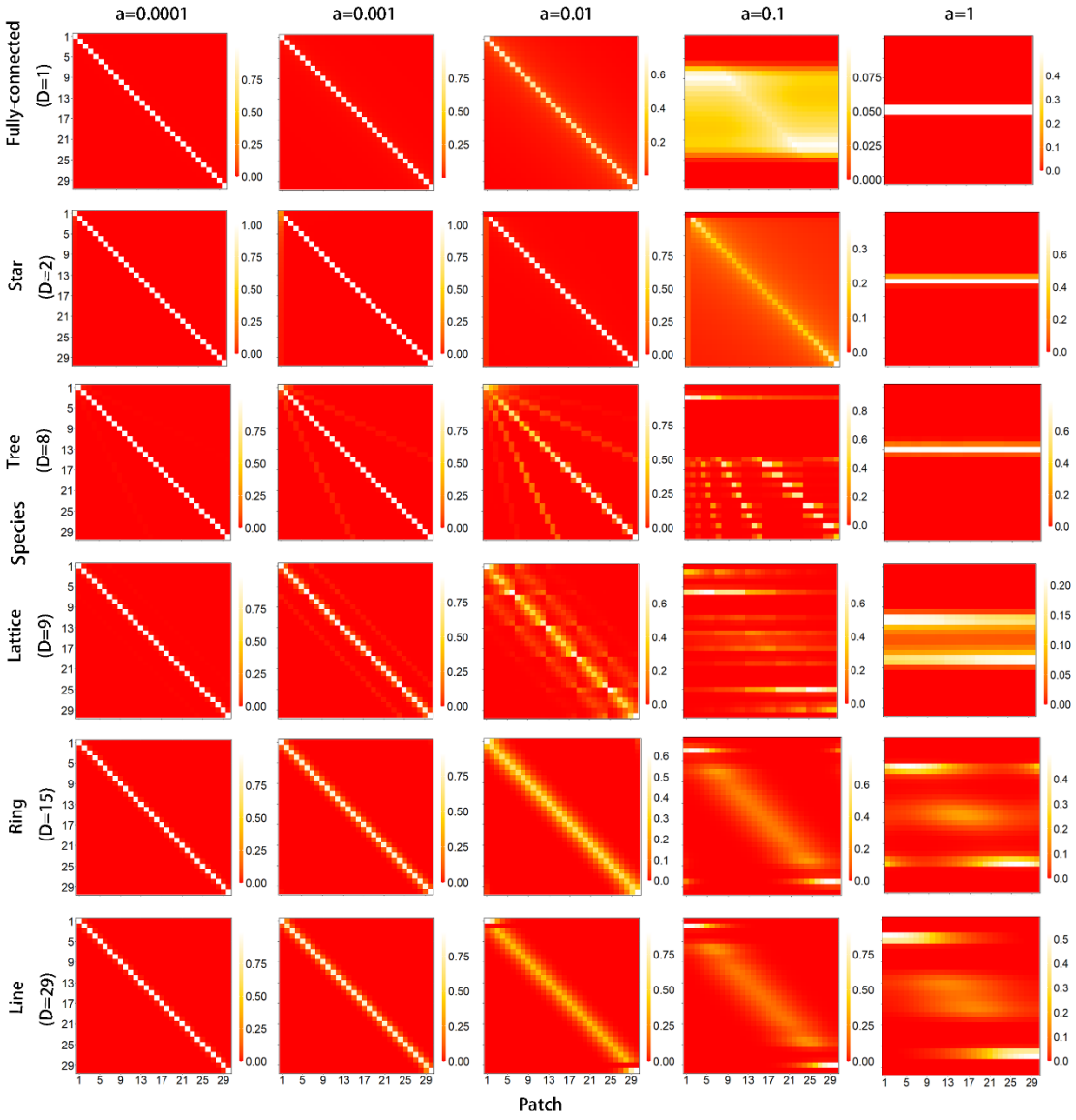
a=0.0001
a=0.001
a=0.01
a=0.1
a=1
Fully-connected (D=1)
Star (D=2)
Tree (D=8)
Species
Lattice (D=9)
Ring (D=15)
Line (D=29)
Patch

Figure 2

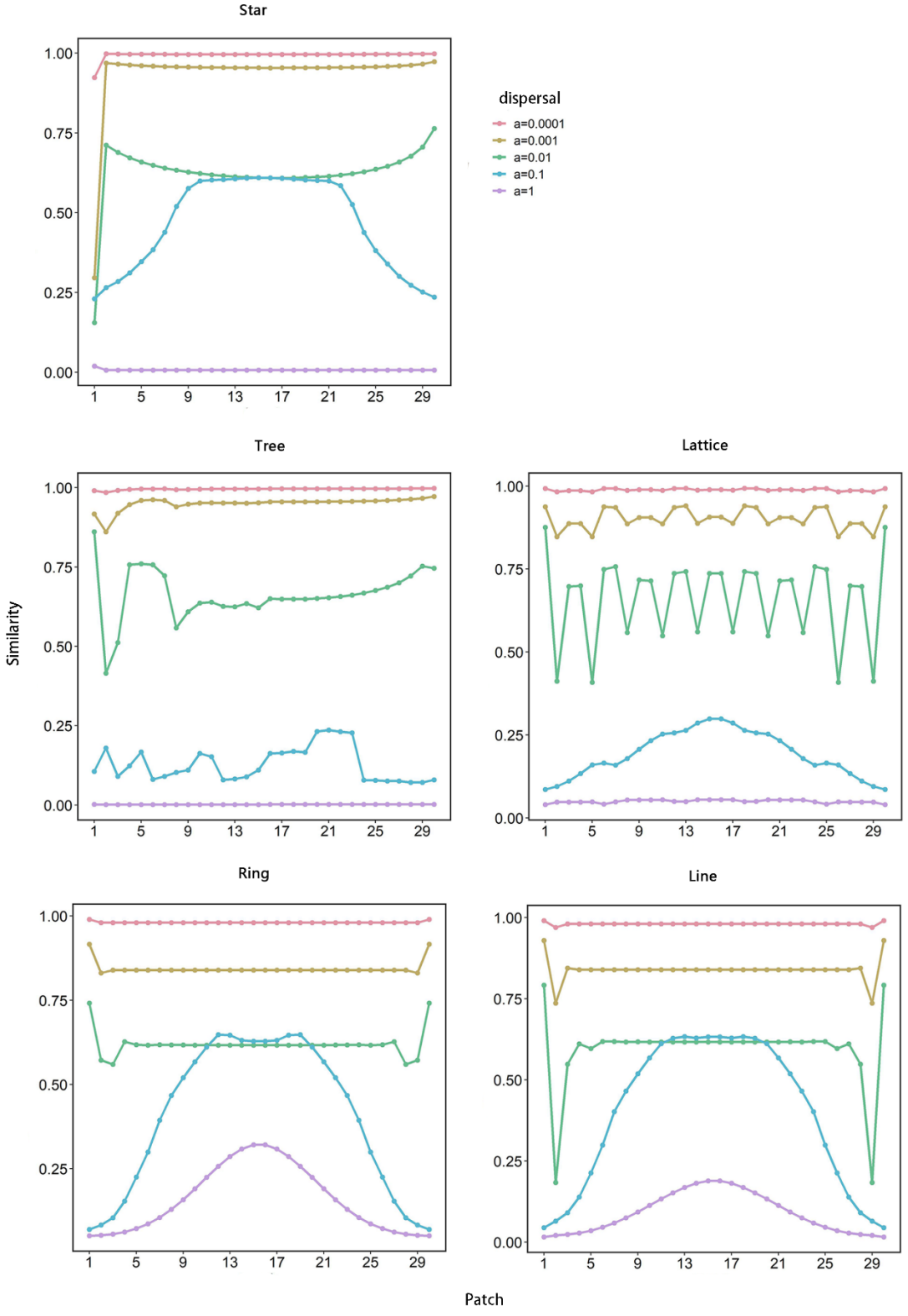

562

563 Figure 3

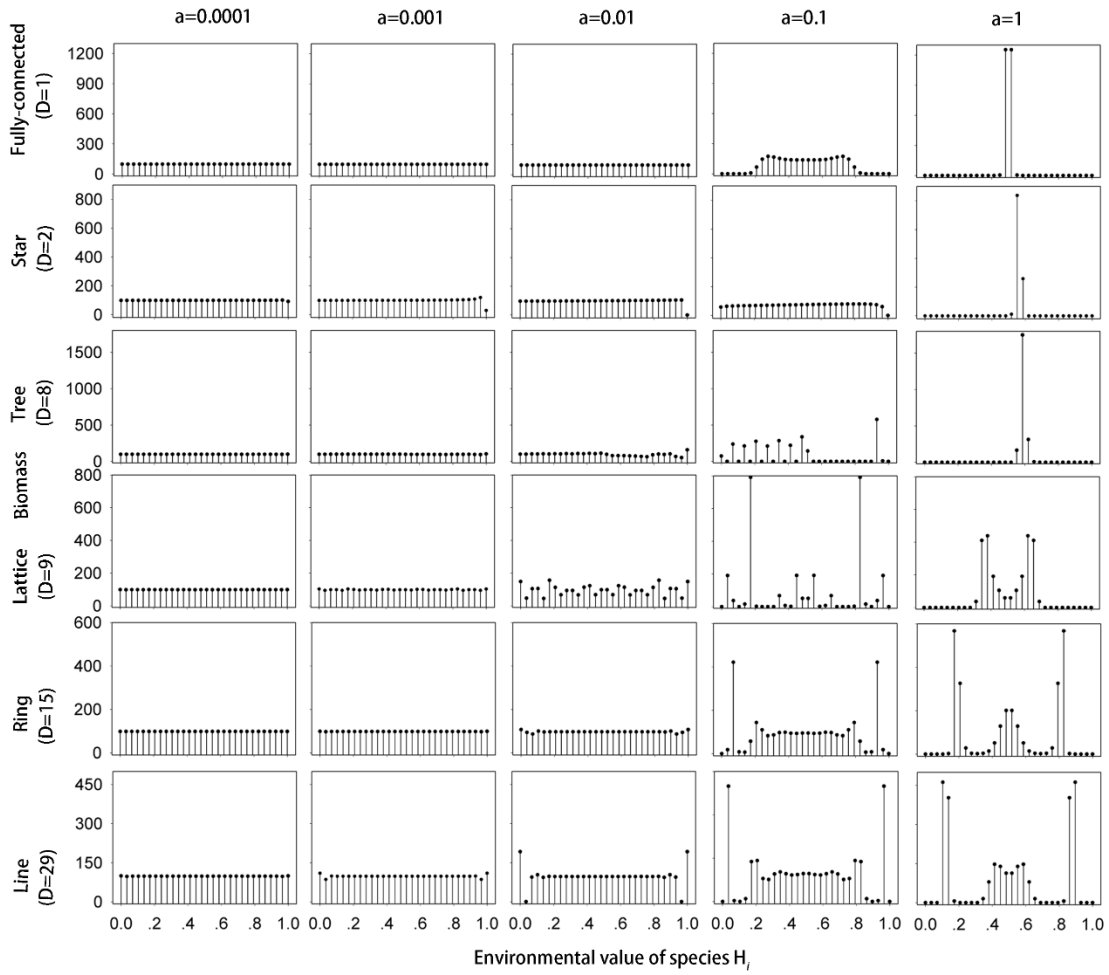
a=0.0001
a=0.001
a=0.01
a=0.1
a=1
Fully-connected (D=1)
Star (D=2)
Tree (D=8)
Biomass
Lattice (D=9)
Ring (D=15)
Line (D=29)
Environmental value of species H_i

Figure 4

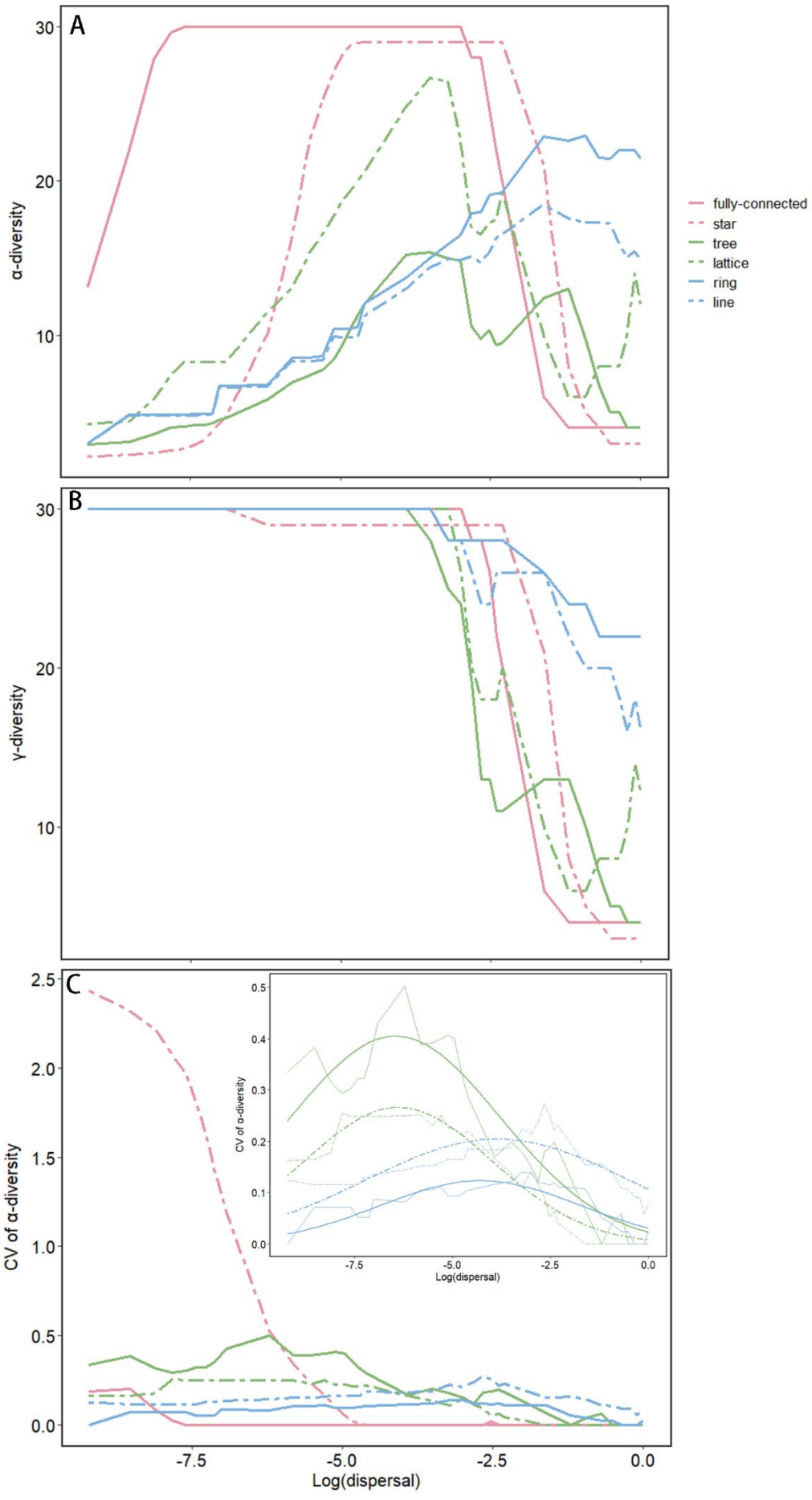
A
α-diversity
30
20
10
B
γ-diversity
30
20
10
C
CV of α-diversity
2.5
2.0
1.5
1.0
0.5
0.0
-7.5
-5.0
-2.5
0.0
Log(dispersal)
CV of α-diversity
0.5
0.4
0.3
0.2
0.1
0.0
-7.5
-5.0
-2.5
0.0
Log(dispersal)
fully-connected
star
tree
lattice
ring
line

568

569 Figure 5

570

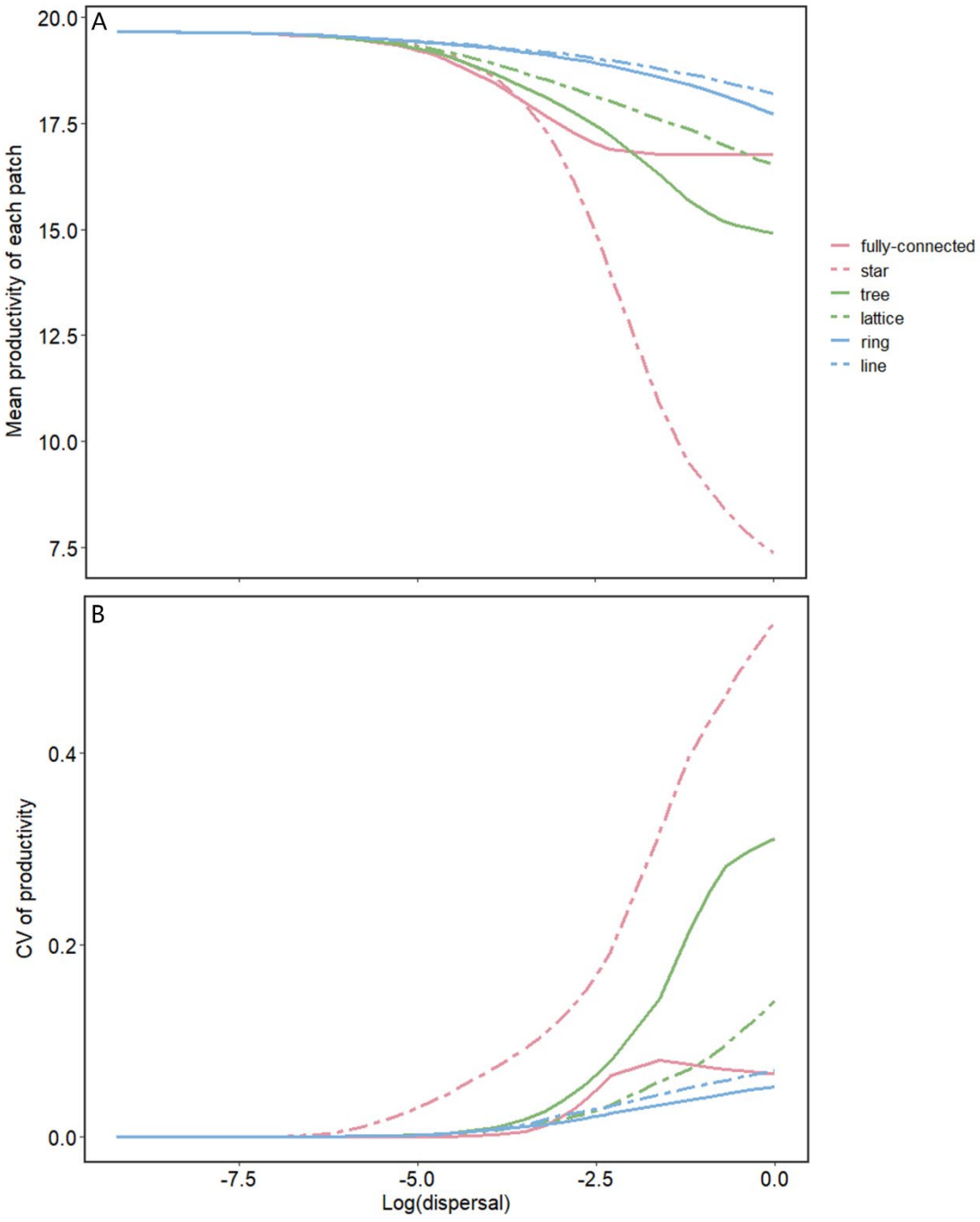

571

572 Figure 6